Quantitation of Hindered Rotations of Diphenylhexatriene in Lipid Bilayers by Differential Polarized Phase Fluorometry

Abstract. *Diffusional motions of 1,6-diphenyl-1,3,5-hexatriene (DPH) were observed by differential polarized phase fluorometry. The measurements indicated that the depolarizing rotations of DPH in propylene glycol are isotropic. The results in vesicles of dimyristoyl-L-α-phosphatidylcholine indicated that diffusional rotations of DPH are dominated by hindered torsional motions. Combined use of both differential phase and steady-state anisotropy measurements showed that the average rotational angle of DPH, at times long compared to the fluorescence lifetime, is limited to about 23° at temperatures below the transition temperature of the lipid and that these rotations become less hindered above the transition temperature. The evidence that the depolarizing rotations of DPH in a lipid bilayer are different from those in an isotropic solvent calls into question the meaning of membrane microviscosity as determined by fluorescence anisotropy.*

Measurements of the fluorescence polarization of probes embedded in lipid bilayers have been widely used to estimate the microviscosity of the hydrophobic regions of both natural and model cell membranes (*1–6*). In these microviscosity measurements it is assumed that the depolarizing rotational motions of the probe in lipid bilayers are equivalent to those in isotropic solvents.

1,6-Diphenyl-1,3,5-hexatriene (DPH) has become widely used in microviscosity studies because of its favorable fluorescence polarization and spectral properties (*7*), but perhaps more importantly because of the dramatic changes in fluorescence polarization that occur at the solid-liquid phase transition temperature of phospholipid bilayers (*8, 9*). These strongly temperature-dependent polarization changes are sharper with DPH than with other fluorophores, such as 12-anthroyl stearate, 1-anilino-8-naphthalenesulfonic acid, perylene, and *N*-phenyl-1-naphthylamine. A presumed advantage of DPH is the fact that the absorption and emission oscillators both lie along the long axis of the fluorophore. As a result, only rotations perpendicular to this long axis will be effective in depolarizing the fluorescence emission. For these reasons, steady-state polarization measurements with DPH are considered to accurately describe the microviscosity of lipid bilayers.

Recent studies involving time-resolved decays of fluorescence anisotropy have demonstrated that DPH undergoes only hindered torsional motions below the phase transition temperature of dimyristoyl-L-α-phosphatidylcholine (DMPC) vesicles and that there is a highly nonexponential decay of anisotropy above the transition temperature (*10*). These phenomena reflect a hindered environment for DPH in lipid bilayers and illustrate the need to understand the types of probe motion that are responsible for fluorescence depolarization so that polarization data can be interpreted in terms of the membrane microviscosity.

In the work reported here we used differential polarized phase fluorometry to investigate the rotational diffusion of DPH in an isotropic solvent and in DMPC vesicles. This technique was used recently (*11, 12*) to study the rotational rates of fluorophores in isotropic solutions. Differences in the phase angle of the vertical and horizontal components of the emitted light are measured when the fluorescence sample is irradiated with polarized, sinusoidally modulated light. The tangent of the phase difference between the vertical and horizontal components of the fluorescence emission (tan Δ) is a function of the fluorescence lifetime (τ), the fluorescence anisotropy (*13*) value in the absence of rotational diffusion (r_0), the rotational rate in radians per second (R), and the circular modulation frequency (ω), as shown by Eq. 1

$$\tan \Delta = \frac{(2R\tau)\omega\tau r_0}{m(1 + \omega^2\tau^2) + (2R\tau/3)(2 + r_0) + (2R\tau)^2} \quad (1)$$

where

$$m = \frac{1}{9}(1 + 2r_0)(1 - r_0) \quad (2)$$

The quadratic form of Eq. 1 may be used to obtain R from measurements of tan Δ.

$$(2R\tau)^2 + (2R\tau)\left(\frac{2 + r_0}{3} - \left|\frac{r_0}{\tan \Delta}\right|\omega\tau\right) + m(1 + \omega^2\tau^2) = 0 \quad (3)$$

For isotropic rotations the maximum value possible for tan Δ (tan Δ_{max}) is a function of only r_0, ω, and τ.

$$\tan \Delta_{max} = \frac{3\omega\tau r_0}{(2 + r_0) + 6[m(1 + \omega^2\tau^2)]^{1/2}} \quad (4)$$

Equations 1 to 4 apply to spherical molecules or isotropic rotators. If the rotational motions are isotropic the tan Δ_{max} values will agree with that predicted

Table 1. Differential polarized phase measurements of 1,6-diphenyl-1,3,5-hexatriene. Fluorescence lifetimes and differential phase lifetimes were measured by the phase shift method (*12, 16*), using a modulation frequency of 30 MHz. To obtain lifetimes unbiased by depolarizing Brownian rotations the excitation and emission polarizers were set 0° and 55° from the vertical, respectively (*17*). The instrumental conditions were: excitation wavelength, 360 nm; excitation filter, Corning 7-54; emission filters, Corning 3-73 and 2 mm of 1*M* $NaNO_2$. All equipment was from SLM Instruments, Inc. Steady-state anisotropy and anisotropy values in the absence of rotational diffusion (r_0) were obtained directly in a subnanosecond spectrofluorometer with the radio-frequency electronics and light modulation turned off. Rotational rates of DPH in propylene glycol were determined both by solving Eq. 3 and by steady-state anisotropy measurements. In the latter case we used the Perrin-Weber equation, $r_0/r = 1 + 6R\tau$. We found $r_0 = 0.392$ at −57°C and used this value in all our calculations. The lifetimes shown in this table are those observed at the temperature corresponding to the maximum value of tan Δ. The synthetic lipid DMPC (Sigma) was used without further purification. Chromatography of the phospholipid on silica with chloroform, methanol, and water (65:25:4) and ethyl ether, benzene, ethanol, acetic acid, and water (40:40:20:8:4) showed a single spot by both phosphate and dichromate char staining. The DMPC vesicles were prepared by adding benzene solutions of the probe and lipid to a stainless steel beaker, with a probe/lipid molar ratio of 1:500. The benzene was evaporated by gently warming the solution while maintaining a constant flow of argon over the materials. Buffer (0.01*M* tris, 0.05*M* KCl, *p*H = 7.5) was added to the dried lipid to establish a concentration of 0.17 mg of lipid per milliliter of buffer. Solutions were sonicated with a Heat Systems model 350 sonicator at 200 W, using a 0.5-inch-diameter tip. The temperature of the solution was maintained near 40°C during the 15-minute sonication period. This preparation was annealed for 1 hour at 40°C and then centrifuged at 48,000*g* for 90 minutes. No significant fluorescent impurities were observed in unlabeled vesicles prepared in an identical manner. No scattered light at the excitation wavelength or at the Raman wavelength was observed through the filters used for the lifetime and differential lifetime measurements. The absorbance of DPH in propylene glycol was 0.4 at 360 nm. A blank solution of propylene glycol showed no significant fluorescence at equivalent instrumental conditions.

Sample	τ (nsec)	tan Δ_{max}		Percentage of tan Δ_{max} observed
		Observed	Calculated	
Propylene glycol	4.5	0.185	0.195	95
DMPC vesicles	8.7	0.159	0.278	57

0036-8075/78/0623-1399$00.50/0

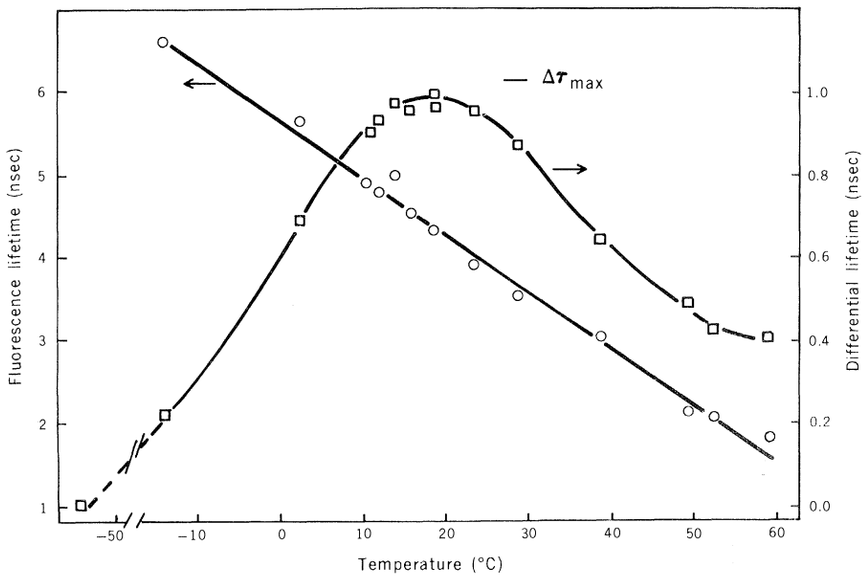

Fig. 1. Fluorescence lifetimes and differential polarized phase lifetimes of DPH in propylene glycol.

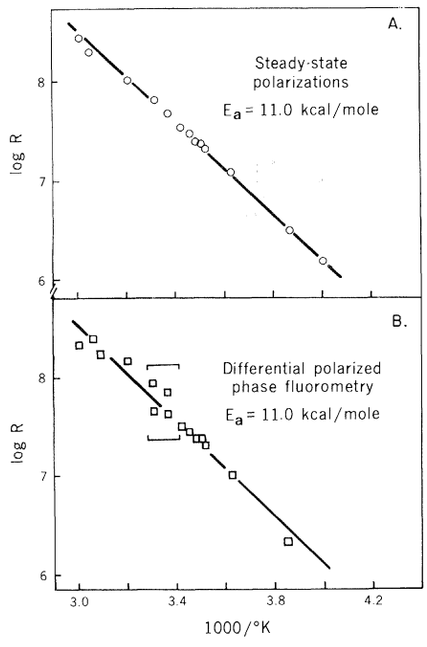

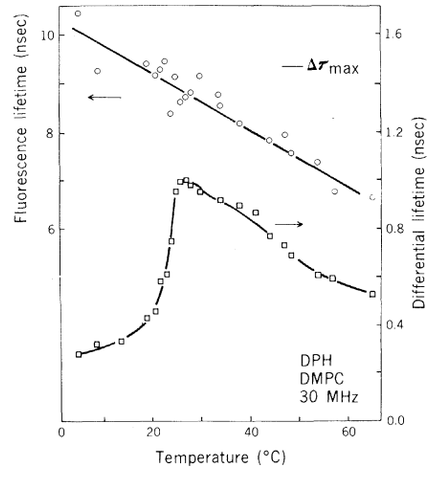

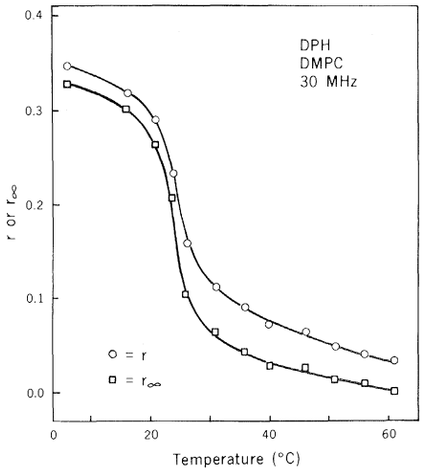

Fig. 2 (top left). Rotational rate of DPH in propylene glycol. Rotational rates were calculated by both steady-state polarization measurements (A) and differential polarized phase fluorometry (B). The duplicate points between the bars in (B) result from the two possible solutions to Eq. 1. Near $\Delta\tau = \Delta\tau_{max}$ the choice of the proper solution is not clear. However, the value chosen is often unimportant since the rotational rates are similar. Fig. 3 (bottom left). Fluorescence lifetimes (○) and differential polarized phase lifetimes (□) of DPH in DMPC vesicles. The $\Delta\tau_{max}$ indicates the maximum differential lifetime predicted for a free isotropic rotator with $r_0 = 0.392$ and $\tau = 8.7$ nsec. Fig. 4 (above). Limiting anisotropy values for DPH in DMPC vesicles. Limiting anisotropy values (□) were calculated from Eqs. 9 to 11, using data from Fig. 3 at regular temperature intervals, and from the steady-state anisotropy values (○). By using data read off Fig. 3, we effectively smoothed the data and minimized errors resulting from single data points. There are two solutions for r_∞ at each point because Eq. 11 is quadratic. However, in each instance one of the rotational rates was negative and thus inadmissible.

by Eq. 4. Anisotropic rotations, a heterogeneous population of isotropic rotators, or hindered torsional motions result in a tan Δ_{max} less than that predicted by Eq. 4. Studies of Mantulin and Weber (*12*) demonstrated the usefulness of differential polarized phase fluorometry in the detection of anisotropic rotations.

Figure 1 shows the fluorescence lifetimes and differential phase lifetimes of DPH in propylene glycol ($\omega\,\Delta\tau = \tan\Delta$). The precise agreement of the maximum value of the differential tangent with the theoretical value (Table 1) demonstrates that the depolarizing rotations of DPH in propylene glycol are isotropic. Additional evidence for this is provided by the precise agreement between the rotational rates calculated from the differential phase measurements and those calculated from the steady-state polarization measurements using the Perrin-Weber equation (Fig. 2; see the legend of Table 1 for a description of the experimental procedures).

Figure 3 shows the differential polarized phase measurements of DPH-labeled DMPC vesicles. Similar results were obtained with unsonicated liposomes (*14*). These results demonstrate an increase in the rotational or torsional motions of DPH at the phase transition temperatures, but in contrast to the results with DPH in propylene glycol the maximum differential tangent is only 57 percent of the theoretical value predicted by Eq. 4. This 43 percent tangent defect is greater than that predicted by Mantulin and Weber (*12*) for any degree of rotational anisotropy in the depolarizing motions. Since the depolarizing rotations of DPH are likely to be isotropic (*7*) and a similar tangent defect was observed in unsonicated liposomes of DMPC (which provide a more homogeneous population of probe molecules), we concluded that the tangent defect we observed was a result of hindered torsional motions of the probe when located in the lipid bilayer.

Recently, Weber (*15*) obtained solutions for the differential tangent under conditions where the rotational motions of the probe are limited to a nonzero anisotropy value (r_∞) at times long compared to τ. Under these conditions the parallel $[I_\parallel(t)]$ and perpendicular $[I_\perp(t)]$ components of the fluorescence emission are given by

$$I_\parallel(t) = (1 + 2r_\infty)\exp(-t/\tau) + 2(r_0 - r_\infty)\exp\left[-\left(\frac{1}{\tau} + 6R\right)t\right] \quad (5)$$

$$I_\perp(t) = (1 - r_\infty)\exp(-t/\tau) - (r_0 - r_\infty)\exp\left[-\left(\frac{1}{\tau} + 6R\right)t\right] \quad (6)$$

From these equations Weber (*15*) obtained

$$\tan \Delta = \omega \tau (r_0 - r_\infty)(2R\tau)/\{m(1 + \omega^2\tau^2) + (2R\tau/3)[2 + r_0 - r_\infty(4r_0 - 1)] + (2R\tau)^2(1 + 2r_\infty)(1 - r_\infty)\} \quad (7)$$

and

$$\tan \Delta_{max} = \omega \tau (r_0 - r_\infty)/\{1/3[(2 + r_0) - r_\infty(4r_0 - 1)] + 2[m(1 + 2r_\infty)(1 - r_\infty)(1 + \omega^2\tau^2)]^{1/2}\} \quad (8)$$

For $r_\infty = 0$, Eqs. 7 and 8 reduce to forms applicable to free isotropic rotations.

Since r_∞ is a measure of the degree to which the depolarizing rotations of DPH are restricted, we wished to use our measurements to obtain r_∞ in DMPC bilayers at various temperatures. Differential phase measurements alone do not yield r_∞. However, in a hindered environment both the steady-state anisotropy and the differential tangent are functions of r_∞ and R. With these measurements and the fluorescence lifetime it should be possible to determine r_∞ and R. By integrating and normalizing Eqs. 5 and 6 over times from 0 to infinity we obtained

$$r_\infty = r + \frac{(r - r_0)}{6R\tau} \quad (9)$$

Substituting Eq. 9 into Eq. 7 gives

$$(C \tan \Delta)(2R\tau)^2 + (D \tan \Delta - A)(2R\tau) + (E \tan \Delta - B) = 0 \quad (10)$$

where

$$A = 3B = \omega\tau(r_0 - r)$$
$$C = (1 + 2r)(1 - r)$$
$$D = 1/3(2r - 4r^2 + 2) \quad (11)$$
$$E = C/9 + m\omega^2\tau^2$$

By measuring tan Δ, r, and τ, one can obtain R from Eq. 10. This value of R may then be substituted into Eq. 9 to calculate r_∞. The values for r_∞ so obtained are presented in Fig. 4. It is apparent from these data that DPH is highly hindered at temperatures below the transition temperature of the bilayer ($r_\infty \simeq 0.3$) and that DPH rotates freely above the transition temperature ($r_\infty \simeq 0$). The midpoint of the change in r_∞ occurs at 24°C, which is near the phase transition temperature (*8*).

Using time-resolved decays of fluorescence anisotropy, Chen *et al.* (*10*) found $r_\infty \simeq 0.25$ below the transition temperature and $r_\infty \simeq 0.01$ above the transition temperature. Our results are in excellent agreement with those of Chen *et al.* However, the rapidity with which differential tangents may be measured allowed us to obtain a complete temperature profile for r_∞ (Fig. 4). Thus differential phase fluoreometry will be a powerful method for investigating hindered motions of fluorophores in lipid bilayers.

The detection of restricted diffusional motions of DPH in lipid bilayers illustrates the difficulties inherent in the extrapolation of DPH fluorescence anisotropy data to estimate membrane microviscosity. In such extrapolations it is assumed that the depolarizing rotations of DPH in the bilayers are identical to those in the reference solvent, which is usually a mixture of branched-chain alkanes. Our data demonstrate that this assumption is not valid, a result that calls into question the definition of membrane microviscosity from anisotropy measurements. Combined steady-state anisotropy measurements and differential phase fluorometry more accurately describe the rotational motions of probes in lipid bilayers and provide a better understanding of the constraints imposed by an anisotropic lipid bilayer. By such experiments it should also be possible to select fluorescence probes whose rotational motions in lipid bilayers are similar to those in homogeneous solutions, and thereby provide a better method for estimating membrane microviscosities.

J. R. LAKOWICZ
Freshwater Biological Institute and
Department of Biochemistry, University of Minnesota, Navarre 55392
F. G. PRENDERGAST
Department of Pharmacology, Mayo Medical School, Rochester, Minnesota 55901

References and Notes

1. M. Shinitzky, A. C. Dianoux, C. Gilter, G. Weber, *Biochemistry* **10**, 2106 (1971).
2. U. Cogan, M. Shinitzky, G. Weber, T. Nishida, *ibid.* **12**, 521 (1973).
3. C. L. Brashford, C. G. Morgan, G. K. Radda, *Biochim. Biophys. Acta* **426**, 157 (1976).
4. K. Jacobson and D. Wobschhall, *Chem. Phys. Lipids* **12**, 117 (1974).
5. N. F. Moore, Y. Barenholz, R. R. Wagner, *J. Virol.* **19**, 126 (1976).
6. M. Shinitzky and M. Inbar, *J. Mol. Biol.* **85**, 603 (1974).
7. M. Shinitzky and Y. Barenholz, *J. Biol. Chem.* **249**, 2652 (1974).
8. B. R. Lentz, Y. Barenholz, T. E. Thompson, *Biochemistry* **15**, 4521 (1976).
9. ———, *ibid.*, p. 4529.
10. L. A. Chen, R. E. Dale, S. Roth, L. Brand, *J. Biol. Chem.* **252**, 2163 (1977).
11. G. Weber, *J. Chem. Phys.* **66**, 4081 (1977).
12. W. W. Mantulin and G. Weber, *ibid.*, p. 4091.
13. Fluorescence polarization (P) and anisotropy (r) may be interconverted by using $P = 3r/(2 + r)$. Fluorescence anisotropy is defined by
$$r = \frac{I_\parallel - I_\parallel}{I_\parallel + 2I_\perp}$$
where $I_\parallel$ and $I_\perp$ are the time-averaged values of $I_\parallel(t)$ and $I_\perp(t)$. The limiting anisotropy r_∞ is related to the average angle (ϕ) to which torsional motions are restricted at times long compared to the fluorescence lifetime by $r_0/r_\infty = 2/(3\cos^2\phi - 1)$. It is important to recognize that r_∞ is a measure of the average angle, and not a measure of the maximum angle through which the fluorophore rotates.
14. J. R. Lakowicz and F. G. Prendergast, unpublished observations.
15. G. Weber, *Acta Phys. Pol.*, in press.
16. R. D. Spencer and G. Weber, *Ann. N.Y. Acad. Sci.* **158**, 361 (1969).
17. ———, *J. Chem. Phys.* **52**, 1654 (1970).
18. We thank the Freshwater Biological Research Foundation, and especially its founder, R. Gray, Sr., without whose assistance this work would not have been possible. We also thank D. Hogen for valuable technical assistance. The generous support of the American Heart Association, the Mayo Foundation, and the National Institutes of Health under grants ES GM 01238-01A1 (to J.R.L.) and CA 150 83-00 (to F.G.P.) is acknowledged. J.R.L. is an established investigator of the American Heart Association. Our special thanks are due to G. Weber for having supplied us with the theory of hindered rotations (as yet unpublished), and for his continuous generous support of this work.

8 November 1977; revised 18 January 1978

Comparison of Rhapidosomes and Asbestos Microfibrils

Abstract. *Rhapidosomes (cylindrical nucleoprotein rods of bacterial origin) show great structural similarity to the microfibrils of chrysotile asbestos when negatively stained and observed with the electron microscope. If the negative stain is omitted, the asbestos retains its structural detail whereas the rhapidosomes appear to be unstructured bodies. When the microscope is adjusted into a selected area diffraction mode, the asbestos shows characteristic electron diffraction patterns whereas the rhapidosomes appear to be amorphous to electron diffraction.*

Rhapidosomes were first described by Lewin (*1*) who noted that they appeared to be hollow rods roughly 200 by 30 nm. Subsequent workers have identified rhapidosomes in at least 12 different species of bacteria. Although their origin is still obscure, their biochemical structure has suggested that they may arise from cell membranes as the bacteria undergo lysis (*2*). Correll and Lewin (*3*) have emphasized the remarkable similarity of the physical and chemical properties of rhapidosomes to those of tobacco mosaic virus. We describe here observations on the similarity of rhapidosomes to the microfibrils of chrysotile asbestos and suggest methods whereby the two may be distinguished.

While studying bacterial ultrastructure, we observed numerous rod-shaped bodies on the grid surface separate from the bacterial sections. They were cylindrical in shape and had a central core which in some instances protruded from the main body of the rod, characteristics common to rhapidosomes. Although these rods had somewhat larger diameters than many of the reported rhapido-

0036-8075/78/0623-1401$00.50/0